A Remote Sensing Biogeochemical Survey in and around the Linghou Cu- polymetal Deposit, Southeastern China

Ling Han, Chengyan Du*
School of Geology Engineering and Geomatics, Shaanxi Key Laboratory of Land Consolidation and Rehabilitation, Chang'an University, Middle-section of Nan'er Huan Road, Xi'an, 710064, China.
Email: dcychdedu@163.com.

Keywords: The Linghou deposit, biogeochemistry, the OLI image, foliage

Abstract: Using the Landsat 8 imagery and the field- measured vegetation spectra, a biogeochemical survey in the Linghou ore field of eastern China was conducted. Findings indicated that no vegetation anomalies were observed in the 5 to 4 ratioing image. From the perspective of spectral feature, plants within the Linghou diggings, especially at the tailings pond and wastewater pool, "grow worse" than at the peripheries, although several individual exceptions behave against this trend. Thus we should not ignore the local pollution which might be a valuable cue for the concealed ore- bodies or ecological destruction.

1 INTRODUCTION

Remote sensing technology relies mostly on the capability of the sensor to register spectral signatures and other geological features related to mineral deposits (Cavalli et al., 2009). The identification of sites with likely occurrence of hydrothermal alteration is a positive clue for existence of associated ore minerals. Nevertheless, it is not providing a necessary spectral resolution to identify specific minerals because of the broad band configuration of TM/ETM+, particularly in SWIR. The Linghou deposit surveyed in this paper is located in northwestern Zhejiang province, southeastern China, widely covered by vegetation even in winter, but abundant in copper- polymetal deposits. Because of the very dense cover of regolith and vegetation, an alternative approach of survey that reduces the effect of this thick coverage must be developed in order to expose the alteration zones and the anomalies associated with the concealed ore body (Sabins, 1999).

According to (Sims and Gamon, 2002), a series of vegetal physiological and ecological variation, e.g., leaf temperature, chemical component, pigment and water content, etc., may occur in response to ore geochemical anomaly coming from rocks and soils on which plants growth heavily relies. Normally such a toxic action caused by metal poisoning of plants and/or other ecological stresses is twofold: i) The red- shift and/or blue- shift, e.g., chlorophyll normally has a significant absorption within the red-spectral region, while vegetal mesophyll has a remarkable near infrared scattering, and the red-edge appears in between. Generally those poisoned leaves in gold ore- field have a bluely shifted red-edge position (Kooistra et al., 2004). In addition, spectral red- shift associated with a declined content of leaf water due to contamination of heavy- metals also occurs. ii) Relative to the healthy canopy, poisoned vegetal leaves may always have higher brightness in the images. Due to a very thick sedimentary- vegetation cover in this area, concealed rocks and deposits have become the focus of mineral exploration; and in this regard, the study on plant spectrum and its link to (environmental or metallogenetic) geochemical anomalies may make a particular contribution, although these characteristics are just an indirect reflection of mineral occurrence and environmental destruction.

From the above, the objective of this article is to conduct a remote sensing data- driven biogeochemical survey in Linghou ore field, eastern China.

Han, L. and Du, C.
A Remote Sensing Biogeochemical Survey in and around the Linghou Cu- polymetal Deposit, Southeastern China.
In *Proceedings of the International Workshop on Environment and Geoscience (IWEG 2018)*, pages 273-282
ISBN: 978-989-758-342-1

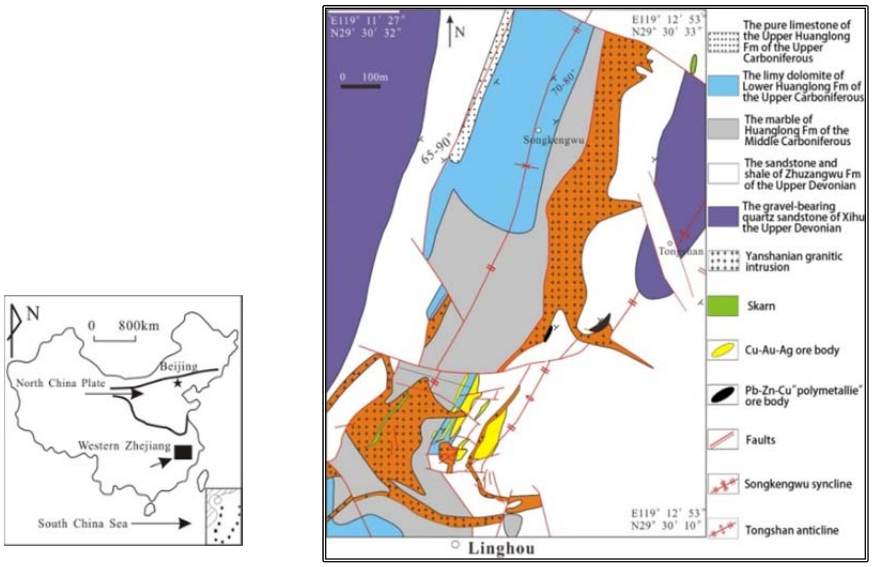

Figure 1: Geological sketch map of the Linghou polymetallic deposit.

2 GEOLOGICAL SETTING

The Linghou deposit (119°11′45″E, 29°29′30″N) is located in the western Zhejiang province of China. It is a medium- scale Cu- Pb- Zn deposit whose genesis type is known as the hydrothermal reworked deposit, as shown in Figure 1. The surrounding strata of this deposit are mainly upper Devonian and middle to upper Carboniferous along with the general strike of NE- SW. There are two ore blocks in Linghou: Songkengwu and Linghou (Tang et al. 2015). Typical calc- silicate (skarn) alteration can be only found in the Songkengwu ore- field. Phyllic alteration characterized by disseminated sericite and quartz, with minor pyrite and chalcopyrite is well developed within the granites. Silicification characterized by quartz in ores or quartz + pyrite + chalcopyrite veins in strata and granites is closely linked to Cu- Au- Ag mineralization (Zhang et al. 2013). The carbonate alternation, characterized by earlier recrystallization of dolomite + calcite associated with the Cu- Pb- Zn minerali- zation, and later calcite clusters in a hydrothermal calcite cave near the ore- bodies, and calcite (± galena) veins/veinlets across the ore and granites, is also quite common.

3 DATA COLLECTION AND PRETREATMENTS

The multispectral image was collected from Landsat 8 OLI_TRIS digital products (spatial resolution: 30 m) that are freely downloadable from http://glovis.usgs.gov/. Its Row/Path is 40/119, the time of acquisition is 14-04-2013. Later in Mar. 2016, a series of data were collected from vegetation leaf samples in and around the mine area. The sampling location is threefold: 1, sampling within the mine excavations; 2, sampling within the peripheral or background area relative to diggings, acting as a control group; 3, sampling in one or more kindred deposit (s) nearby in order to make a contrast. Using FieldSpec®4 HI- RES spectrograph, the reflectivity curve of dozens of leaf samples were tested in- situ. The spectral measurement of foliage adhered strictly to the user's guide of this apparatus. The basic approach of data quality control is to do radiometric calibration by keeping the probe vertically orienting the horizontally placed whiteboard which is an approximate Lambertian reflector with a fixed and known reflectivity (Hatchell, 1999). Particularly, if the weather

condition was not as good as expected, the frequency of calibration must be doubled— every two minutes. Conversely, it would be the best if a 100% reference line of reflectivity could be obtained in sunny days.

Several pre- treatments, like imagery cutting, radiometric calibration, atmospheric correction, and orthorectification were carried out. At the same time, waters with NDVI (Normalized Difference Vegetation Index) between -0.079 and 0.05 were erased for subsequent analysis, which accounts for about 27.19% of the total area. There is no need to mask other objects like settlements, (concrete/asphalt) roads, factory buildings, etc., for they are too small to extract and have limited influence on the analysis.

4 SPECTRAL ANALYSIS OF VEGETATION COVER

4.1 Spectral Analysis

(Zhao et al. 2017) discovered that on the 1: 200000 stream- sediments geochemical map, there is a significant copper (Cu) - polymetal anomalous zone lying in and around this studied area, e.g., copper content in its concentration center (119°11′47.88″E, 29°29′05.07″N) reaches up to 3358×10-6 ppm, nearly 120 times higher than copper clarke number (Rudnick and Gao, 2003). According to (Gan and Wang 2004), a significant decline of chlorophyll pigment is the most obvious visual sign of vegetation poisoned by ore metals. In this respect, it is believed that the band combination 5, 4 and 3 of Landsat 8 OLI is typically applied for vegetation analysis, and seemingly, intense red color represents vigorous growing plants producing a lot of chlorophyll, while lighter shades of reds are still vegetation, but may either be mature trees/plants or dead, unhealthy plants. Unfortunately, the composite results seem not so ideal: most light red shades are actually montanic shadowed outcrops, or to a lesser extent sparse vegetation areas (Ghasemloo et al., 2011). A similar scenario can apply to the NDVI or band 5 to 4 ratioing imagery.

In the visible wavelengths, there are several peaks of spectral absorption and reflection (e.g. a blue trough at ~480 nm, a red trough at ~680 nm, and a green peak at ~550 nm), sensitively associated with foliage content of chlorophyll. The OLI band 5 at NIR has a striking platform of reflection, relative to any other peaks of reflection between 1400 and 2500 nm, whose average reflection is normally greater than or equal to ~70% and related to moisture content. Inasmuch the 5 to 4 ratioing OLI image should play a role extracting biogeochemical anomalous information relating to metal toxic action. In SWIR: OLI band 6 (1560~1660 nm) and band 7 (2100~2300 nm) are quite sensitive to foliage moisture content and mesophyll cellular structure. Figure 2 shows the darkest pixels in the OLI 5/4 ratio image, which, in theory, represents the unhealthy vegetation. But in reality, they are just a reflection of hill- shaded areas.

According to (Tong 1988), the Linghou mine is considered to be a sedimentary- transformed stratabound type. The syngenetic sediments may be rich in Cu and other ore metals, but far from mineral industrial grade. The Cu- polymetal- enriched sandy shale layer is located mainly in -50 m and deeper underground.(Cheng et al. 2012) pointed out that the covering layer plays an essential role in shielding and attenuating ore elemental migration, so that the deep- rooted geochemical anomalies and metal-logenesis exhibit only gentle and low grade anomalies at the surface. However, due to a special geochemical property, it is reported that Cu abundance in soils at the upper part of the copper deposit comes up to n000 ppm, which can be used for secondary- halo prospecting (Liu et al., 1980). Also local edaphic geochemical or vegetal anomalies related to ore (Jiang et al., 2002) in Linghou mine were confirmed (Yang et al., 2009). Table 1, e.g., shows that the average abundance of Cu in the Linghou diggings is significantly greater than normal 5 ppm. As the relevant anomalies cannot be exposed in Figure 2, so we have to turn our focus to local and limited stressing phenomena related to mine pollution, which is probably beyond the monitoring ability of OLI imagery.

4.2 Vegetational Hyperspectral Analysis

Although the vegetational coverage severely masks/alters surface signals related to metallogenic alteration and environmental deterioration, we cannot exclude the possibility that by feat of spectral sampling under similar illumination conditions, vegetation information affected more or less by various stressing agencies, and hence could act as an indicator serving to get some specific anomalies

associated with mineralization in this area (Ma, 2000).

Table 1: The biogeochemical anomalies (concentrations of Cu and Zn in the plant leaves) in the Linghou and adjacent Fuyang mining areas[a].

Site	Species	Cu (mg kg^{-1})	Zn (mg kg^{-1})
Residue sand place	Polygonum lapathifolium	150.2	505.6
	Alternanthera sessilis	220.3	280.2
	Eclipta prostrata	125.7	525.6
Farmland	Siegesbeckia glabrescens	190.1	95.4
	Eclipta prostrata	235.4	750.4
Old mining area	Elsholtzia splendens	687.0	530.3
	Rumex acetosa	530.0	530.3
	Artemisia lavandulaefolia	198.6	372.5
	Viola diffusa	606.4	585.6

[a] After (Jiang et al., 2002).

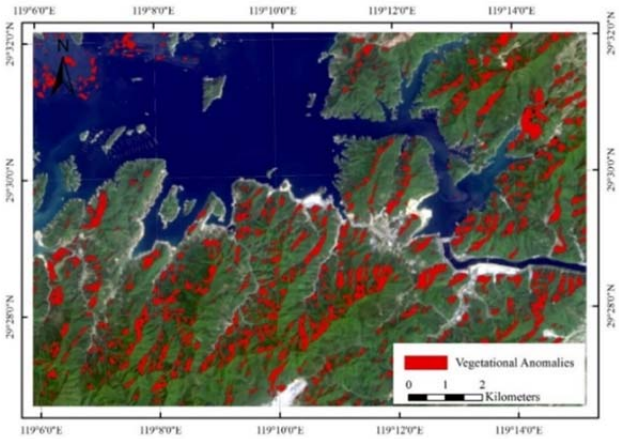

Figure 2: The darkest colored areas in the OLI 5/4 ratio image, namely the so- called vegetation anomalies. The relevant threshold was determined by visual interpretation.

Figure 3: The sampling position P-2 at the periphery of mine (29°29′16.56″N, 119°11′ 41.76″E). The main lithology in this profile is carbonate- rock formation (C2h), within this limestone wall no conspicuous quartz mines and granitic apophyses were found. Here the withered Miscanthus floridulus leaves were collected for spectral analysis.

4.2.1 Phyllostachys Pubescens

Phyllostachys pubescen is one of the most important cash crop in western Zhejiang province, but most phyllostachys pubescens in later March are not in their vigorous growth period, and many leaf edges look still withered yellow. Four samples of phyllostachys pubescen leaves were collected in three sites. Two of them are at the mine (noted as PP at O-1, and O-2), while the other two acted as the comparative samples, as shown in Figure 3, are at the periphery of mine (PP at P-1, and P-2). P-1 is closer to the diggings than P-2. O-1 is at a small catchment basin (29°29′17.04″N, 119°12′5.69″E), and it was sampled close to the surface runoffs, ensuring that the plants root system nearby can absorb enough ore metals related to mineralization. O-2 was collected at 29°29′21.19″N, 119°11′52.34″E. P-1 was tested at 29°29′21.06″N, 119°12′4.87″E. This site is on a hillside adjacent to the mining area, and there is no surface runoff, ore-bearing quartz veins and outcropped bed- rock

nearby. These samples are fresh and plausibly healthy leafage, leaving out partly withered or newly transplanted plants. The weather condition during test was cloudy to sunny.

As seen in Figure 4, the reflectance curves of these 4 samples are similar in shape but distinct in numerical magnitude, so spectral ratioing (or derivative) is the best way to eliminate these effects. For example, the average of foliage reflectance between 850 and 880 nm, which is just the spectral region of band 5 of an OLI image, is noted by B5 here; while the average between 640 nm and 670 nm, namely the spectral region of band 4, is noted as B4 here; and the ratios of B5 to B4 of PP at O-1 is 8.12, O-2 is 7.18, P-1 is 10.78, and P-2 is 6.84. Apparently, the growth conditions of O-1 and O-2 in diggings site are inferior to P-1; the phyllostachys pubescen tree at P-2, however, grows in a little pile of regosol within a small limestone sink- hole; so it seems that the subalimentation, not the biotic stress associated with ore contamination, may be responsible for its lower value of B5/B4, which is in accordance with (Jiang et al. 2013) report that calcareous soils are characterized by neutral/slightly- alkaline chemistry, thinner soil layer, lack of available moisture, and etc., and few wood species in them could grow well. Additionally, (Li 2007) pointed out that due to polymetal stressing, foliage reflection within 550~680 nm must be enhanced significantly, that is why the reflectivity of PP at P-1 and P-2 seems low.

Figure 5 further demonstrates the 1st order derivative reflectivity between 680 and 750 nm: the derivative of PP at P-1 reflectivity peaks at 719 nm, known as the red- edge (Rock et al., 1988). Relative to P-1, there seems a significant blue- shift of PP red- edges at O-1 (701 nm) and O-2 (702 nm). PP red- edge at P-2 is 700 nm. The slopes of the red-edge are 0.0073 (O-1), 0.01093 (O-2), 0.005344 (P-1) and 0.008896 (P-2), respectively, and PP at P-1 therein is the most gentle one. Actually, variation in chlorophyll and carotenoid concentrations, in addition to a buildup of additional pigments such as tannins, may occur within leaves in response to stress like heavy- metal pollution in the mining area, and a blue- shift phenomenon may always act as a diagnostic signature helping to identify the biogeochemical damage caused by metallic stress agents (Ninomiya et al., 2005). However, due to a relatively small amount of spectral shifts (versus a relatively larger spectral resolution of the spectrograph), the observation error of discrete spectra, and the spectrum rebuilding error, the red-edge position are not so accurate sometimes, and thus the utilization of this parameter must be considered with cautions.

Another important parameter describing vegetational anomalies is the so called “band-depth”. As displayed in Figure 6- a, taken a foliage sample at O-1 as instance, the reflectance with continuum removed is noted as R’, and the band-depth (D) at each point is calculated by D = 1 - R’ (Sanches et al., 2014). Meanwhile, in order to eliminate the effects of topography, landforms, and atmosphere, and for ease of comparison, normalized band- depth Dn was further worked out by Dn = D / Dc, where Dc is the band- depth of the central band, which, in this work, is assigned the maximum of D within a wavelength range of 350 to 1500 nm. In this way, a continuum- removed reflectance curve is normalized to a range of 0~1.0 that can enhance the vegetal absorption and reflection spectrum. In Figure 6, only the first three peaks of absorption are taken into account in this paper, the first two appearing in visible region: the blue trough and the red trough, and the other one developing in near-infrared range and reflecting foliage moisture. Because of the blue- or red- shift possibly existing, the depths and position of these peaks may not be fixed.

As listed in Table 2, for the first peak, the band-depths of PP at O-1, O-2, and P-2 are significantly greater than at P-1, implying a deepened trough of absorption; also, there is a blue- shift of PP from P-1 to O-2 and P-2. For the third peak, PP at O-2 and P-2, relative to P-1, seem shifted bluewards, and actual band- depths of O-1, O-2, and P-2 are much deeper than P-1. This feature seems not completely consistent with the phenomena that foliage badly stressed by metals may have a saliently shallowed band- depth.

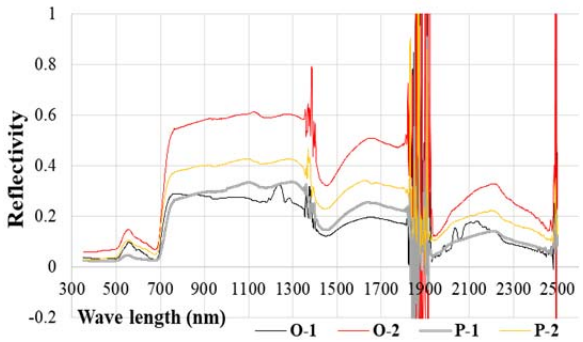

Figure 4: Spectral curves of reflectance of four phyllostachys pubescen leafage Samples. Note that there is a drastic fluctuation around 1900 nm, which may have something to do with the illumination conditions and the surroundings like breeze.

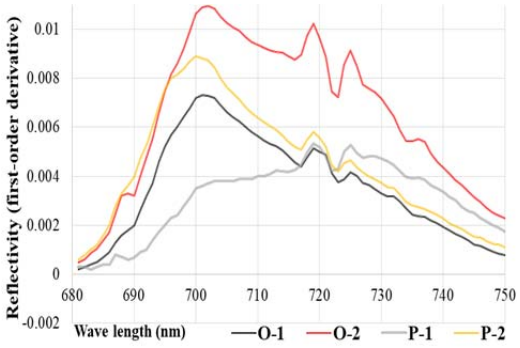

Figure 5: The 1st- order derivative reflectivity (680~750nm) of 4 phyllostachys pubescen samples.

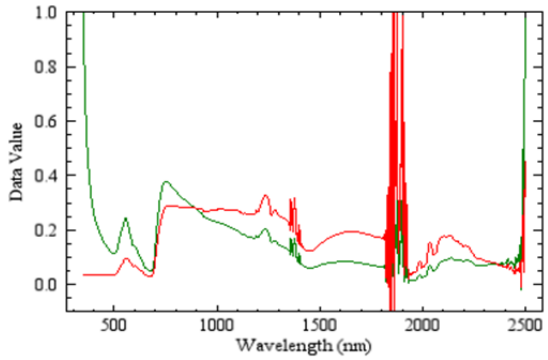

Figure 6: (a) The reflectivity curve of sample O-1, the red curve: initial reflectivity curve (for both (a) and (b)), and the green one: the continuum- removed curve of reflectivity.

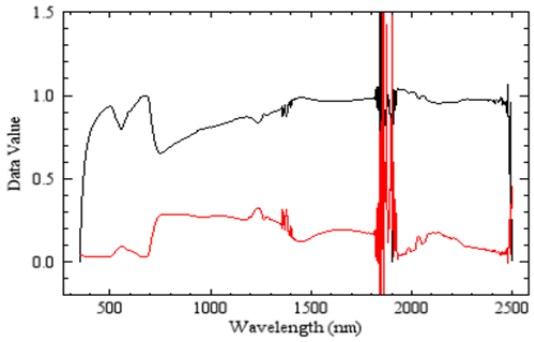

Figure 6: (b) Normalized band- depth of O-1 (the black line).

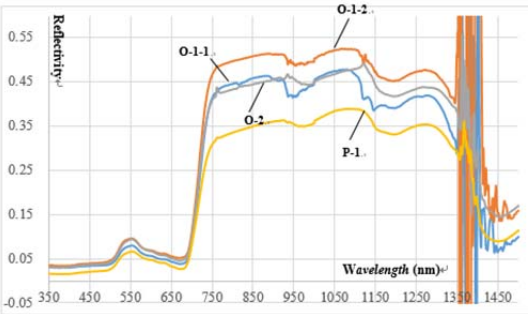

Figure 7: Spectral curves of reflectance of four fir leafage samples, and the corresponding sample description is seen in the context.

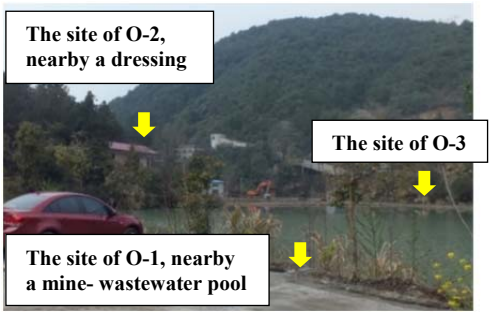

Figure 8: The central position of sampling sites of O-1, O-2 and O-3.

Table 2: The band- depth at three troughs of absorption of all the foliage samples in Linghou mine[a].

	Site	Species	Band- Depth						"Band 5/4"	The red- edge	
			WL	peak-1	WL	peak-2	WL	peak-3		Slope	WL
GROUP I	0-3	NU-1	550	0.948	759	1	1650	1.051	1.164	0.002	720
	0-3	MF	490	0.975	678	1	1454	1.011	3.481	0.013	696
	0-3	IC	502	0.986	676	1	1453	1.006	3.706	0.004	719
	0-2	M	498	1	678	1	1459	1.006	5.048	0.007	695, 696
	0-1	MF	498	0.957	679	1	1368	1.035	5.292	0.008	721
	P-1	Arbutus	505	0.999	680	1	1457	1	5.529	0.006	719
	0-2	M	440	0.992	679	1	1459	1.002	5.665	0.009	696
	0-1	MF	494	0.987	675	1	1456	0.999	6.423	0.023	719
	P-2	PP	493	0.981	675	1	1454	0.990	6.742	0.009	700
	0-3	OT	497	0.983	675	1	1458	1.001	6.925	0.015	719
	0-3	PP	501	0.977	678	1	1458	0.992	7.102	0.011	701, 702
GROUP II	Site	Species	WL	peak-1	WL	peak-2	WL	peak-3	"Band 5/4"	Slope	WL
	0-1	PP	499	0.933	677	1	1461	0.987	7.727	0.007	701, 702
	0-2	NU-2	496	0.977	678	1	1460	1.002	8.062	0.020	701
	0-1	OT	502	0.994	675	1	1463	1.001	8.870	0.010	719
	0-2	F	495	0.978	675	1	1459	1.001	8.956	0.010	719
	0-1	F	497	0.999	672	1	1356	1.063	9.089	0.011	719
	0-2	NU-3	496	0.992	676	1	1452	1	9.497	0.013	719
	0-3	MP	496	0.984	673	1	1458	1.004	9.810	0.014	719
	P-1	PP	500	0.890	673	1	1460	0.892	10.650	0.005	719, 725
	P-1	F	492	0.998	675	1	1453	1	10.851	0.007	719
	0-1	F	498	0.988	674	1	1360	1.511	10.852	0.010	721
	0-3	NU-4	498	0.994	674	1	1456	0.999	10.922	0.014	701
	0-1	NU-5	498	0.994	673	1	1455	1	11.070	0.013	719
	0-2	CT	499	0.973	676	1	1460	0.990	11.115	0.013	719
	P-1	OT	502	0.991	678	1	1457	1.003	11.473	0.012	719
	0-1	MF	498	0.999	671	1	1399	1.408	11.698	0.005	719, 720
	0-3	NU-6	502	0.986	672	1	1454	1	12.092	0.013	719
	0-3	NU-7	490	0.992	675	1	1455	1.001	12.846	0.011	719
GROUP III	Site	Species	WL	peak-1	WL	peak-2	WL	peak-3	"Band 5/4"	Slope	WL
	0-1	Loquat	494	0.952	673	1	1360	4.794	18.629	0.009	719
	P-2	Loquat	497	0.987	674	1	1454	0.990	18.781	0.011	719
	P-1	Arbutus	498	0.997	676	1	1449	1	19.190	0.002	721
	P-2	OT	497	0.980	673	1	1451	0.989	19.481	0.014	719
	P-1	Citrus	500	0.995	669	1	1457	0.997	20.393	0.014	719

[a] Note: The average of foliage hyperspectral reflectance between 850 and 880 nm is noted as band 5 (also the spectral range of Band 5 of an OLI image), while the average between 640 and 670 nm, namely the spectral range of Band 4 of an OLI image, is noted as B4, and the "band- ratioing 5/4" is actually a ratio of B5 to B4, no spectral anomalies can be observed in the image; or the relevant anomlies are submerged into the hill- shaded areas, and hence indistinguishable. O-1, 2, 3 and P-1, 2 stand for different sampling sites, see context for the positions for O-1, O-2, P-1 and P-2. O-3 is at 29°2 9′21.06″N, 119°12′4.87″E. WL is short for "Wave- length", and NU is short for "name known", NU-1 therein is a newly grown leaf. Due to my limited professional knowledge on phytology, some samples were unable to be identified in the open air, most of them, however, were collected from local arbor species. MF- miscanthus floridulus, IC- incense cedar, OT- osmanthus tree, MP- masson pine, PP- phyllostachys pubescen, CT- camphor tree, M- moss, F- Chinese fir. Besides, peak1: between 350nm and 557nm, the maximum value of normalized band- depth and the wavelength it corresponding to; peak 2: between 558 and 750, the maximum of band- depth normalized and the wavelength; peak 3: between 1400 and 1500nm, the maximum band- depth and its position of wavelength.

4.2.2 Cunninghamia Lanceolate

Cunninghamia lanceolate is commonly called Chinese fir. Evergreen plants can retain chlorophyll even under freezing conditions (Yokono et al., 2008), so fir samples here may provide a better spectral comparison. Four foliage samples of Chinese fir were collected. The first two were sampled at O-1, noted by F at O-1-1 and O-1-2, the third one is noted by F at O-2, and the fourth one, noted by P-1, was tested in the periphery of mine. As shown in Figure 7, P-1 of Chinese fir has the lowest reflectivity as expected; and "band ratios 5/4" of F at O-1-1 (10.9757), O-1-2 (9.21867), and O-2 (9.086264) are simultaneously less than P-1 (11.0689). Between 650 and 750 nm, a shift of the steep slope to shorter wave- lengths (blue- shift) is seen in reflectance data of O-1-1, O-1-2, and O-2 relative to P-1; while between 1250 and 1450 nm, it shifts towards the longer wave length direction (red- shift). There is no obvious change of the red- edge inflection point of these fir samples, while the slope of the red- edge of F at P-1 is gentler (0.007).(Ma 2000) had related changes in the slope of the red- edge (700~740 nm) to chlorophyll concentrations in the foliage, and both the position and slope of the red- edge will change as healthy leaves progress from active photosynthesis through metals- induced stresses and various stages of senescence (natural decline) due to loss of chlorophyll and the addition of tannins.

In addition to the curves of normalized band- depth from 350 nm to 1500 nm, for the first peak, there is a significant red- shift of F at O-1-1 (498 nm), O-1-2 (497 nm) and O-2 (495 nm), relative to P-1 (491 nm); meanwhile, F at P-1 has a slightly greater and lower value of band- depth (0.996181, Dc here used for normalization is assigned the maximum of band- depths within 350 to 1200 nm) than the other three: O-1-1: 0.977587, O-1-2: 0.998518, O-2: 0.955699; for the second peak, there are blue- shifts of O-1-1 (674/675 nm), O-1-2 (673 nm) and O-2 (676 nm), relative to P-1 (677 nm); for the third peak, F at O-1-1 and O-1-2 are ignored, while O-2 (1459 nm) relative to P-1 (1452 nm) appears a 5 nm red- shift, but the actual band- depths of them have little difference. Like phyllostachys pubescen (PP), these features are basically consistent with the phenomena of foliage poisoned more or less by ore heavy- metals (Xu et al., 2003).

4.2.3 Other Plants

From Table 2 which is a list of spectral parameters of some other foliage samples collected at Linghou, We noticed that there are many individual exceptions behaving against the general pattern summarized above, whereas the "ratioing 5/4" (B5/B4) seems relatively stable, and have a characteristic feature dividing original foliage samples into several distinctive groups, e.g., lower damage site and higher damage site (Rock et al., 1988), although, admittedly different species may correspond to different "ratioing 5/4" values as seen in Table 2.

As manifested in Table 2, the first group includes the first 11 samples within the diggings, adding two anomalous samples at the periphery. The second group is composed of fifteen samples, three of them, i.e., phyllostachys pubescen, fir, and Osmanthus tree, were collected outside the mine, and the remainders are all from the mining district. The relatively healthy third- one has five samples; four of them were sampled at P-1 and P-2, adding one sample of loquat from O-1. As exhibited in Figure 8, the sites O-1, 2, and 3 were sampled nearby the contaminated zones, so the spectral anomalies, as a response to trace metals stressing, in group I and II must be an inevitable phenomenon. Fortunately, parametric characteristics of several leaf samples in group II and III imply that severe destruction of ecosystem in the Linghou ore deposit which is adjacent to the famous Qiandaohu International Tourism Area seems limited in scale and slighter in degree, identified with the findings revealed in the OLI multispectral image. On average, leaf samples within the diggings, as a whole, do have a relatively lower B5/B4 ratio: the average of "ratio 5/4" of peripheral samples (P-1 and P-2) 13.7 is much greater than that of the samples within the mining district (O-1, -2 and -3) 8.6. Likewise, the average of spectral reflectivity between 350 and 1300 nm may also act as a diagnostic parameter reflecting the overall degree of metals stressing, and we found that the average value of this parameter of peripheral samples 0.34 is still a bit greater than that of the samples at the mine 0.26.

Table 2 further reads that: for peak 1, the average band- depth in group I is 0.980455, in group II is 0.980118, and group III 0.9822. Obviously, the depths of absorption in group I and II becomes shallower. For peak 2, the average wavelength position of Group I, Group II and Group III is

684.73 nm, 674.53 nm and 673 nm, respectively. From I to II, and III, there is an obvious blue- shift. The average wavelength position of the red- edge of foliage in group I is at 709.6 nm, in group II is 716 nm, and in group III 719.4nm, this is a blue- shift process also, in accord with the spectral characteristics of vegetation under metal stressing. For peak 3, the median of the wavelength position of samples in group I is 1457 nm, in group II is 1456 nm, and group III 1451 nm, indicating a red- shift. Herein the substitution of average for median is operated for suppressing the drastic fluctuations of the reflectivity curve (appearing from time to time) from 1400 to 1500 nm. Moreover, taking advantage of the OLI image to perform vegetational pollution monitoring, the parameter band- ratioing 5/4 (or NDVI) has merely a 30 m spatial resolution, namely the spectral feature of mixed pixels within a 30 m × 30 m grid, and that is why the statistic mean method was used here to analyze Table 2. Nevertheless, there are many individual exceptions behaving against the overall pattern summarized above.

5 DISCUSSIONS

Although the stress agents responsible for the observed spectral characteristics have not been identified by testing of foliage biochemical components, mine wastewater and surficial tailings ponds do exist within the diggings.(Song et al. 2014) believed that anomaly of RS biogeochemistry has obvious internal identity with soil chemical anomaly in material quantity and quality, although vegetal self- protective mechanism decreasing the absorption of ore metals may be activated. Actually, even in and around the world- class Dexing Mine that is 160km away from Linghou, not every foliage species is metals- enriched, even different parts of one individuality have distinctive metal content (Jiang et al., 2013), let alone those individual exceptions of different tree species sensitive to different metals as well as different sampling sites suffering different degrees of pollution. In Table 2, e.g. Osmanthus foliage at P1 was sampled at a small hillside, while its counterpart at P2 was collected in the agrarian zone, the latter, unlike PP at P-2, has a bit larger 5/4 “ratioing”, and the loquat sample’s ratio at P1 and P2 seems similar. Therefore sample-grouping and group- averaging aforementioned are essential (Zhao et al., 2017). Thus, we practically reconfirmed poisoning metals stressing on local vegetation at Linghou perhaps is too weak to form a characteristic fractal dimension or a specific normally distributed mass by itself, standing out from the drastic difference of brightness and shade hue caused by ruggedness of relief everywhere, but we still need to keep an eye on those small- scaled prospecting and pollutional criteria revealed by plant spectral abnormality.

6 CONCLUSIONS

It is certainly true from the remote sensing data that spectral anomalies can be observed in several leaf samples, especially those collected close to the tailings ponds and the wastewater pools.

With a few exceptions, most of the known samples do not show diagnostic spectral anomalies. For those “exceptional” samples, it is impossible to determine whether the relevant anomalies are related to the ore body and the associated soil heavy- metal contamination, or to other stressing agencies because the leaf biogeochemical measured data is missing.

The biogeochemical remote sensing technology is rarely available in the ore prediction and environment pollution estimation, if there is no display of extensive spectral anomalies in the image. This article provided a counterexample that the biogeochemical RS information should be treated with great caution. The so- called RS biogeochemical anomalies might be untenable, if no further evidence, such as the measured leaf heavy-metal content, can verify their existence. Such anomalies are better to be considered as an auxiliary approach for ore prediction or environmental monitoring, and it provides a good idea of where further research should be on a specific area instead of wasting resources in places where the possibility of any positive findings is very slim. This is what our research is about.

ACKNOWLEDGEMENTS

This work was financially supported by the 1:50, 000 geological mapping in the loess covered region of the map sheets: Caobizhen (I48E008021), Liangting (I48E008022), Zhaoxian (I48E008023), Qianyang (I48E009021), Fengxiang (I48E009022), & Yaojiagou (I48E009023) in Shaanxi Province,

China, under Grant [DD-20160060]. And the project of open fund for key laboratory of land and resources degenerate and unused land remediation, under Grant [SXDJ2017-7].

REFERENCES

Cavalli R M., Laneve G and Fusilli L, et al. 2009 Remote sensing water observation for supporting lake victoria weed management *Journal of Environmental Management* **90** 7

Cheng Q 2012 Ideas and methods for comprehensive prediction of mineral deposits in covered areas *Earth Sciences* **37** 06

Gan F P and Wang R S 2004 Research of the technological methods of extraction of remote- sensing rock and mineral information Beijing: Geological Publishing House (In Chinese)

Ghasemloo N, Mobasheri M R and Rezaei Y 2011 Vegetation species determination using spectral characteristics and artificial neural network (scann) *Journal of Agricultural Science and Technology* **13** 4

Hatchell D C 1999 ASD Technical Guide. 3rd Edition, Analytical Spectral Devices Inc, Boulder

Jiang L Y, Shi W Y and Yang X E, et al. 2002 Cu-hyperaccumulators in mining area Chinese *Journal of Applied Ecology* **13** 7 (In Chinese with English abstract)

Jiang M J, Hu J Q and Si W J 2013 A survey and filtration of copper- enriched plants in Dexing copper mining zone *Jiangxi province Jiangsu Agricultural Sciences* **41** 7(In Chinese)

Kooistra L, Salas E A L and Clevers J G P W, et al. 2004 Exploring field vegetation reflectance as an indicator of soil contamination in river floodplains *Environmental Pollution* **127** 2

Li N 2007 The spectral and image characteristics of vegetation in the press of heavy metal Master's dissertation of Shandong University of Science and Technology (In Chinese with English abstract)

Liu Y J, Cao L M, Li Z L, et al. 1980 Elements geochemistry. Beijing: Science Press (In Chinese)

Ma Y L 2000 Biogeochemical characteristics of the Hetai gold deposit, Guangdong province and their significance in remote- sensing exploration *Acta Mineralogica Sinica* **20** 1 (In Chinese with English abstract)

Ninomiya Y, Fu B and Cudahy T J 2005 Detecting lithology with advanced spaceborne thermal emission and reflection radiometer (ASTER) multispectral thermal infrared "Radiance- at- Sensor" data Remote Sensing of Environment **99** 1-2

Rock B N, Hoshizaki T and Miller J R 1988 Comparison of in situ, and airborne spectral measurements of the blue shift associated with forest decline *Remote Sensing of Environment* **24** 1

Rudnick R L and Gao S 2003 Composition of the continental crust Treatise on geochemistry 3

Sabins F F 1999 Remote sensing for mineral exploration *oregeol rev Ore Geology Reviews* **14** 3-4

Sanches I D, Filho C R S and Kokaly R F 2014 Spectroscopic remote sensing of plant stress at leaf and canopy levels using the chlorophyll 680nm absorption feature with continuum removal *Isprs Journal of Photogrammetry and Remote Sensing* 97

Sims D A and Gamon J A 2002 Relationships between leaf pigment content and spectral reflectance across a wide range of species, leaf structures and developmental stages Remote Sensing of Environment **81** 2

Song C A, Song W and Lei L Q, et al. 2014 Effect of plant physiological ecology factors on the formation of metalliferous deposit biogeochemical anomaly Advances in Geosciences **04** 06 (In Chinese with English abstract)

Tang Y, Li X and Zhang X, et al. 2015 Some new data on the genesis of the linghou Cu- Pb- Zn polymetallic deposit—based on the study of fluid inclusions and C- H- O- S- Pb isotopes Ore Geology Reviews 71 (In Chinese with English abstract)

Tong M X 1988 Minerogenetic mechanism and potential ore- bearing analysis—No.2 ore body of Jiande Copper deposit as an example Geology of Zhejiang 4 2 (In Chinese with English abstract)

Xu R S, et al. 2003 Remote sensing biogeochemistry Guangzhou: Guangdong publishing house of science and technology (In Chinese)

Yang M G, Huang S B and Lou F S 2009 Lithospheric structure and large- scale metallogenic process in Southeast China continental area. Geol. China 36 (In Chinese with English abstract)

Yokono M, Akimoto S and Tanaka A 2008 Seasonal changes of excitation energy transfer and thylakoid stacking in the evergreen tree taxuscuspidata : how does it divert excess energy from photosynthetic reaction center? Biochimica Et Biophysica Acta**1777** 4

Zhang D H, Wang K Q and Zhu Y D 2013 Project paper of "regionally metallogenic regularity and prediction of copper- polymetal deposits in the west- middle section of the Jiang- Shao collision- orogenic belt" Beijing: China University of Geosciences (Beijing) (In Chinese)

Zhao B and Han L, et al. 2017 Ore- and bio- geochemical survey based on the landsat remotely sensed data in and around the Dexing porphyry copper- polymetal ore- field, southeastern China *Journal of the Indian Society of Remote Sensing* 7